To cite this article: Li X, Jiang X L , Hopman H. Spring-supported arch model for predicting hydrostatic collapse strength of flexible riser with layer gap[J/OL]. Chinese Journal of Ship Research, 2019, 14(Supp 2). http://www.ship-research.com/EN/Y2019/V14/ISupp 2/15.

DOI:10.19693/j.issn.1673-3185.01967

Spring-supported arch model for predicting hydrostatic collapse strength of flexible riser with layer gap

*Li Xiao**, *Jiang Xiaoli*, *Hopman Hans*

Department of Maritime and Transport Technology, Delft University of Technology, Delft 2628 CN, Netherlands

Abstract: [**Objectives**]As oil and gas exploration enters the field of ultra-deep water, once the outer structure of the flexible riser is damaged, the inner carcass will carry huge external hydrostatic pressure. As one of the geometric imperfections, the gap between the carcass and pressure amour may cause a significant reduction in the collapse strength of flexible risers, which will lead to the so-called wet collapse. [**Methods**]Aiming at this problem, this paper presents a spring-supported arch model for estimating the collapse strength of a subsea flexible riser with a layer gap, and the wet collapse process of the carcass is divided into pre-contact and post-contact phases. In the pre-contact phase, the instability behavior of the inner carcass is analyzed using the stability theory of single ring structure. When the interlayer gap is closed, the carcass begins to be supported by the pressure armor, and the structure enters the post-contact phase, here the outside pressure amour is considered as springs which support the detached portion of the inner carcass. At the same time, the finite element collapse model is employed to verify the reliability of this spring-supported arch model for a set of gap widths. [**Results**]The predictions of the proposed models agree very well with the numerical results, and the collapse pressure is very sensitive to the stiffness of the pressure amour and layer gap width. When the initial gap width between layers increases from 0 to 0.5 mm, the collapse pressure of the flexible riser will decrease by about 18%. If the tightly fitted carcass is supported by a stiffer pressure amour, the collapse strength will be greatly improved. [**Conclusions**]For a flexible riser with a harder pressure amour and a smaller layer gap, the proposed analytical model can effectively predict its hydrostatic crushing strength.

Key words: flexible riser; critical collapse pressure; layer gap; wet collapse; ultra-deep water

CLC number: U661.42;P751

0 Introduction

A flexible riser is a pipe-like structure which provides conduits for conveying hydrocarbons or injection fluid between wellheads and floaters[1] . A typical flexible riser is made up of multiple layers with different structural and operational functions, as shown in Fig. 1[2]. The metallic layers are designed to take load while the polymeric layers are added as sealing material[3]. Since oil and gas production reaches ultra-deep water fields, flexible risers must be capable of resisting high hydrostatic pressure[4]. When excessive external pressure is applied to a flexible riser, it will collapse, the minimum collapse pressure is called critical pressure[5].

For the most part, critical pressure is determined by considering the most extreme loading conditions of the flexible riser, which is called "wet collapse"[6]. In this scenario, seawater floods the annulus through the breached outer sheath, and the entire external pressure acts directly on the inner liner. The interlocked carcass layer which is encased by the pres-

Received: 2018-11-12 **Revised:** 2019-12-11

Supported by: Fund of China Scholarship Council (201606950011)

Authors: Li Xiao, male, born in 1990, Ph.D. candidate. Research interest: safety assessment of offshore structures based on ultimate strength. E-mail: X.Li-9@tudelft.nl

Jiang Xiaoli, female, born in 1973, Ph.D., associate professor. Research interest: structural integrity assessment of marine structures. E-mail: X.Jiang@tudelft.nl

Hopman Hans , male, born in 1956, master, professor. Research interest: ship design, production and operation. E-mail: J.J.Hopman@tudelft.nl

***Corresponding author:** Li Xiao

sure armour is the main component for collapse resistance in this case. Generally, two collapse modes for the innermost carcass would occur once the collapse failure happens, referred to as the figure-eight-shaped mode and heart mode as shown in Fig. 2[7]. This paper deals specifically with the figure-eight-shaped mode of flexible risers under wet collapse.

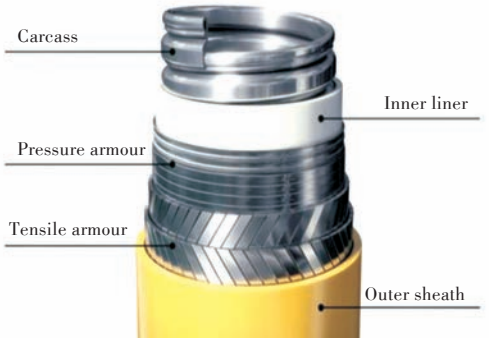

Fig.1 Main component layers of a flexible riser[2]

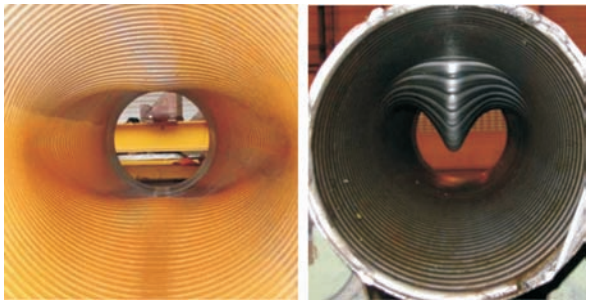

(a) Figure-eight-shaped mode (b) Heart mode

Fig.2 Two collapse modes[7]

Normally, the actual critical pressure is higher than the collapse limit of the carcass because the surrounding pressure armour provides a significant support effect[8]. However, this effect may be reduced by the gap between these two metallic layers. This layer gap, as shown in Fig. 3, is generated in two ways: the volume change of the inner liner or the extrusion of the inner liner into the adjacent interlocked layer[9]. Some researchers have pointed out that the layer gap can cause a significant reduction effect on the critical collapse pressure of flexible risers[9-11].

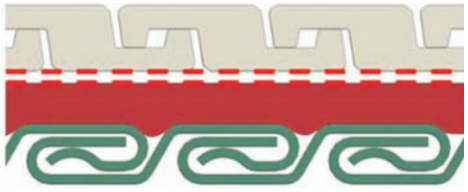

Fig.3 Extrusion of inner liner into adjacent interlocked carcass

To date, most studies related to the layer gap have been limited in numerical investigation, which is less practical for the design purposes of flexible risers. In this paper, a spring-supported arch model is proposed to address the gap-influenced collapse issue. This analytical model can take the width of the gap into account and give a prediction of critical pressure for flexible risers under figure-eight-shaped mode collapse, then the reliability of the proposed model is verified by some case studies.

1 Previous studies

The radial buckling of flexible risers has been studied for years, so analytical models for predicting the critical pressure of flexible risers are mostly developed from ring buckling theories[12]:

$$P_{cr} = \frac{3EI}{R^3} \tag{1}$$

where P_{cr} is the elastic critical pressure of the ring; EI is the bending stiffness of the ring, and E is the elastic modulus, I is the section moment of inertia; R is the ring radius.

Since the flexible pipe is a concentric structure, Glock[13] presented a closed-form analytical solution for the critical pressure of an elastic cylinder confined in a rigid cavity:

$$P_G = \frac{EI}{1-\upsilon^2}\left(\frac{t}{D}\right)^{2.2} \tag{2}$$

where υ is Poisson's Ratio; t is the wall thickness of the cylinder; D is the mean diameter.

Glock's formula was then extended by others to consider tightly or loosely fitted concentric rings[14-15]. Although such formula can consider the gap effect, they give an overestted prediction of critical pressure for flexible pipes. This is because the pressure armour supports the carcass more like an elastic medium rather than a rigid cavity. In this regard, an elastic ring model with horizontal spring supports was proposed as follows[8,16]:

$$P_{cr1} = \frac{3E_iI_i}{R_i^3} + \frac{2}{3}\frac{8E_oI_o}{(\pi^2-7)R_o^3} \tag{3}$$

where P_{cr1} is the critical elastic pressure of the elastic ring; E_iI_i and E_oI_o are the bending stiffness of the inner and outer ring respectively; R_i and R_o are the radius of inner and outer ring respectively.

In the above model, the pressure armour is considered as springs which support the carcass in the horizontal direction, as shown in Fig. 4[8]. However, this model is developed for flexible risers with no gaps between, and only provides an elastic solution due to the usage of the principle of stationary potential energy. Since the flexible risers are more likely to be collapsed in the plastic range under deep-water conditions[16], so efforts are made in this paper to predict the plastic collapse pressure of a flexible riser with a layer gap.

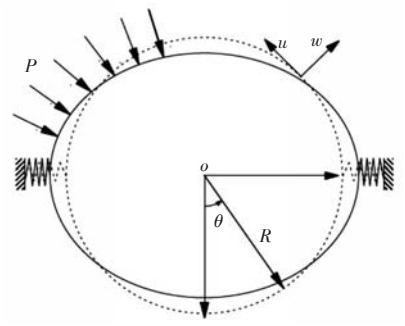

Fig.4 Buckling of inner cylinder with spring supports[8]

2 Analytical model

For the carcass encased in the pressure armour, the radial gap g_w between the two layers is a key element affecting its anti-collapse strength. Intuitively, a larger gap width will lead to a higher reduction of collapse resistance due to the weaker constraints provided by the pressure armour. For a flexible riser which possesses a layer gap between the carcass and pressure armour, its progressive buckling process can be described as in Fig. 5[17].

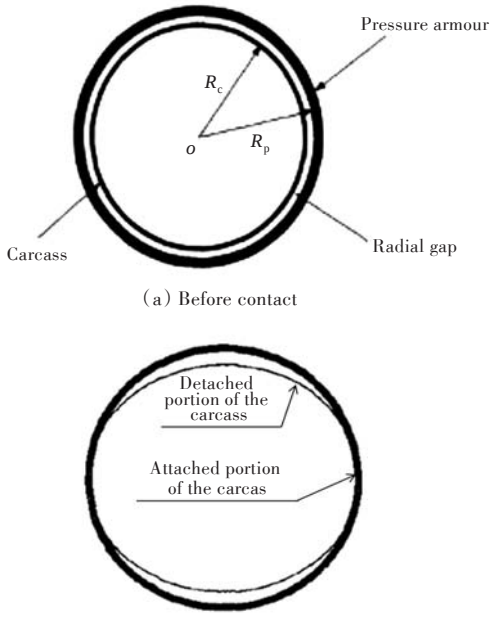

(a) Before contact

(b) After contact

Fig.5 Progressive buckling process for a symmetrical collapse model[17]

It can be seen that two phases occur in this buckling process: the pre-contact and post-contact phases. During the pre-contact phase, the carcass is deformed as a buckled single layer ring. Once contact occurs, the surrounding pressure armour imposes constraints on the inner carcass, so the inner carcass layer can be divided into two portions: the attached portion and detached portion. In the post-contact phase, the collapse pressure of the inner layer is dominated by the buckling strength of the detached portion[18], so the detached portion of the carcass, as shown in Fig. 5, can be separated from the whole carcass and treated as an arch supported by the surrounding pressure armour.

These two phases are considered in the analytical model presented in this section. For the pre-contact phase, formulae related to the radial buckling of a single ring are adopted to determine pressure P_{con} at the contact moment. For the post-buckling phase, the detached portion is regarded as a spring-supported arch which has buckling pressure P_{arch}. The critical pressure of a flexible riser with a layer gap is calculated as the sum of P_{con} and P_{arch}.

2.1 Pre-contact phase

For the buckling of a single ring, Timoshenko et al. [12] assumed that plastic collapse pressure P_y is the value of external pressure at which yielding begins in the extreme fibers of the ring. Therefore, it can be calculated as

$$P_y^2-[\frac{\sigma_y t_c}{R_c}+(1+6\frac{\omega_0}{t_c})P_{cr}]P_y+\frac{\sigma_y t_c}{R_c}P_{cr}=0 \qquad (4)$$

where σ_y is the material yielding stress; R_c and t_c are the mean radius and equivalent thickness of the carcass, and t_c is the equivalent thickness of the carcass which can be calculated according to the Reference [19]; ω_0 is the initial radial deflection of the ring.

Contact moment of a concentric ring structure is shown in Fig. 6, and the maximum horizontal displacement ω_{max} at point A of the plastic collapse pressure is given as

$$\omega_{max}=\frac{\omega_0 P_y}{P_{cr}-P_y} \qquad (5)$$

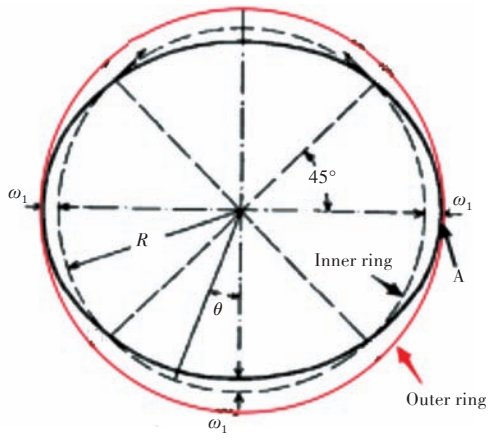

Fig.6 Contact moment of a concentric ring structure

The inner ring will collapse as a single ring if

gap width g_w is greater than ω_{max}; otherwise, layer contact occurs, followed by the post-contact phase. The pressure at the contact moment can be determined by equating the horizontal displacement ω_1 to the gap width g_w. Therefore, this pressure P_{con} at the moment of contact is given as

$$P_{con} = \frac{g_w P_{cr}}{(g_w + \omega_0)} \tag{6}$$

And the bending moment M_{con} and hoop force N_{con} at the crown point of the inner ring can be calculated by

$$M_{con} = P_{con} R_c \frac{\omega_0}{1 - P_{con}/P_{cr}} \tag{7}$$

$$N_{con} = P_{con} R_c \tag{8}$$

And thus, the maximum compressive stress σ_{max} at the crown point for the contact moment is

$$\sigma_{max} = \frac{P_{con} R_c}{t_c} + \frac{6 P_{con} R_c}{t_c^2} \frac{\omega_0}{1 - P_y/P_{cr}} \tag{9}$$

This maximum compressive stress is prepared for the arch model presented in the following post-contact phase.

2.2 Post-contact phase

After the carcass makes contact with the surrounding pressure armour, the contact point will keep moving upwards until the critical pressure arrives, as shown in Fig. 7[17]. During this phase, there is a portion of the inner carcass called the "detached portion" which receives no support from the surrounding pressure armour. The collapse pressure of the flexible riser in the post-contact phase is dominated by the buckling strength of this detached portion of the carcass.

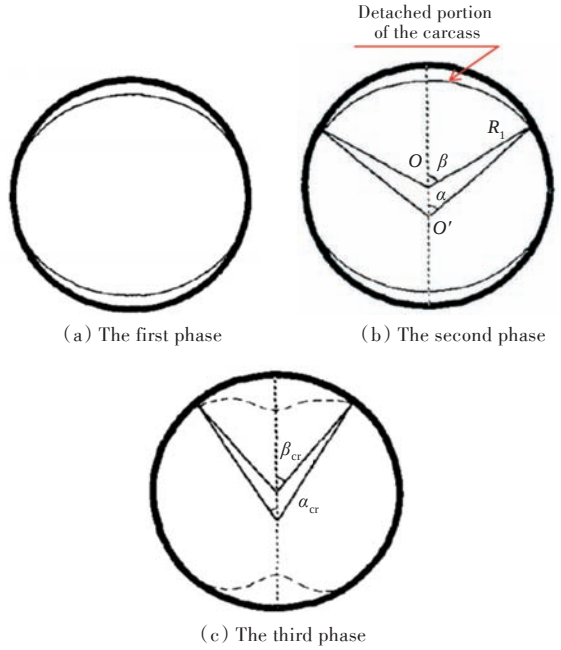

(a) The first phase (b) The second phase

(c) The third phase

Fig.7 Progressive buckling process during post-contact phase[17]

In Fig. 7, the detached portion can be regarded as a circular arch with a new centre O'[17], with its ends restrained by the surrounding pressure armour. In Reference [8], the pressure armour in the proposed model is simplified as two supporting springs at the arch end. In this regard, a spring-supported arch model is proposed, as shown in Fig. 8.

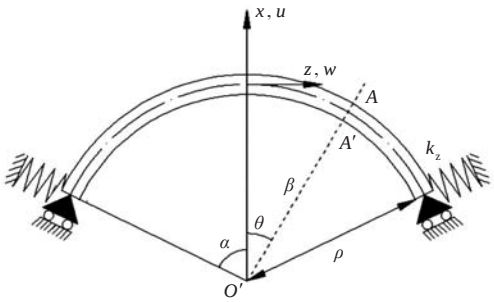

Fig.8 Spring-supported arch model

When the position of the contact point at the collapse moment is determined, the geometry of this circular arch can be calculated by

$$\begin{cases} 2\pi R_c - 2R_{con}(\pi - 2\beta_{cr}) = 4\alpha_{cr}\rho_{cr} \\ \rho_{cr} \sin\alpha_{cr} = R_{con} \sin\beta_{cr} \end{cases} \tag{10}$$

where R_{con} is the distance from the contact point to the ring center O at the collapse moment; α and β are the angular quantities defined in Fig. 7; ρ is the arch radius referred to the new center O'; α_{cr}, β_{cr}, ρ_{cr} are the parameters related to the collapse moment.

The general linear equilibrium equation set for the differential element of such a circular arch is expressed as[20]

$$\begin{cases} Q'_x - N + q_x \rho_{cr} = 0 \\ N' + Q_x + q_z \rho_{cr} = 0 \\ M' + Q_x \rho_{cr} = 0 \end{cases} \tag{11}$$

where M, N, Q_x are the bending moment, hoop force and radial shear force on the differential element; q_x and q_z are uniform loads in the radial direction x and circumferential direction z, as shown in Fig. 9.

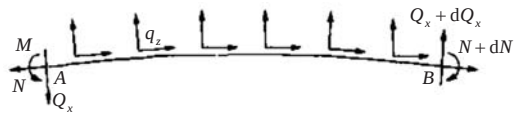

Fig.9 Equilibrium of differential element of arch[20]

In the collapse analysis of flexible risers, the values of the loads q_x and q_z are given as

$$\begin{cases} q_x = -q = -(P - P_{con}) \\ q_z = 0 \end{cases} \tag{12}$$

where q is the differential pressure between external pressure P and pressure at contact moment P_{con}.

The linear relationship between strains ε_x, ε_z,

ε_{xz} and displacements is given as

$$\begin{cases}\varepsilon_x=\dfrac{\partial u}{\partial x}\\ \varepsilon_z=\dfrac{\partial w}{\rho_{cr}\partial\theta}+\dfrac{u}{\rho_{cr}}\\ \varepsilon_{xz}=\dfrac{\partial u}{\rho_{cr}\partial\theta}+\dfrac{\partial w}{\partial x}-\dfrac{w}{\rho_{cr}}\end{cases}\tag{13}$$

where u and w are the displacements of the differential element along the radial and circumferential directions respectively; θ is the angle for an arbitrary cross-section of the arch.

Based on Eq. (12) and Eq. (13), the equilibrium equation set (Eq. (11)) can be redefined:

$$\begin{cases}-E_cA_c\dfrac{w''+u'}{\rho_{cr}}=0\\ E_cA_c\dfrac{w'+u}{\rho_{cr}}+\dfrac{E_cI_c}{\rho_{cr}^3}(u''''+2u''+u)=-Rq\end{cases}\tag{14}$$

where E_c, A_c, I_c are related parameters of the carcass; ()' is a differential calculation, that is $\dfrac{\partial}{\partial\theta}$.

If coefficient K is taken as

$$K=-\frac{\rho_{cr}^3}{E_cI_c}(\rho_{cr}q+E_cA_c\frac{w'+u}{\rho_{cr}})\tag{15}$$

then the general solution of Eq. (14) can be written as

$$\begin{cases}u=KC_1\cos\theta+KC_2\theta\sin\theta+K\\ w=-KC_1\sin\theta-KC_2(\sin\theta-\theta\cos\theta)+KC_3\theta\end{cases}\tag{16}$$

where C_1~C_3 are constants determined by the boundary conditions.

Therefore

$$\begin{cases}M=\dfrac{E_cI_cK}{\rho_{cr}^2}(2C_2\cos\theta+1)\\ N=\dfrac{E_cA_cK}{\rho_{cr}}(1+C_3)+\dfrac{E_cI_cK}{\rho_{cr}^3}(1+2C_2\cos\theta)\\ Q_x=\dfrac{E_cI_cK}{\rho_{cr}^3}(2C_2\sin\theta)\end{cases}\tag{17}$$

For a spring-supported arch model as given in Fig. 8, the boundary conditions are as follows:

1) At crown point $\theta=0$, it should satisfy

$$\begin{cases}u'''+u'=0 & \text{No shear force}\\ w|_{\theta=0}=0 & \text{No hoop displacement}\\ u'=0 & \text{No rotation}\end{cases}\tag{18}$$

2) At the arch end $\theta=\alpha$, it should satisfy

$$\begin{cases}w|_{\theta=\alpha}=0 & \text{No hoop displacement}\\ N_{\theta=\alpha}=R_{con}q & \text{Force equilibrium in hoop direction}\\ Q_x+k_{zp}u=0 & \text{Force equilibrium in rad ial direction}\end{cases}\tag{19}$$

where k_{zp} is the elastic stiffness of the pressure amour, which can be obtained by[16]

$$k_{zp}=\frac{9\pi}{4}\frac{E_pI_p}{R_p^3}\tag{20}$$

where E_p is elastic modulus of the pressure armour; I_p is the section moment of inertia of the pressure armour; R_p is radius of the pressure armour.

The boundary conditions displayed in Eq. (19) are based on a basic assumption made by Jacobson[21]: the thrust force in the attached portion is constant and equals $R_{con}q$. With the above boundary conditions, the formula of C_1~C_3 can be derived:

$$\begin{cases}C_1=\dfrac{D_5}{D_6}-\dfrac{D_4}{D_3D_6}k_{zp}\\ C_2=(\dfrac{D_1}{D_3}+\dfrac{C_1\cos\alpha_{cr}}{D_3})k_{zp}\\ C_3=\dfrac{C_1\sin\alpha_{cr}+C_2(\sin\alpha_{cr}-\alpha_{cr}\cos\alpha_{cr})}{\alpha_{cr}}\end{cases}\tag{21}$$

Now the coefficients in Eq. (21) can be calculated as

$$\begin{cases}D_1=\dfrac{E_cA_c}{\rho_{cr}}\\ D_2=\dfrac{E_ci_c}{\rho_{cr}^3}\\ D_3=(2D_2-k_{zp}\alpha_{cr})\sin\alpha_{cr}\\ D_4=D_1\dfrac{\sin\alpha_{cr}-\alpha_{cr}\cos\alpha_{cr}}{\alpha_{cr}}+2D_2\cos\alpha_{cr}\\ D_5=-(\dfrac{R_{con}q}{K}+D_1+D_2)\\ D_6=D_1\dfrac{\sin\alpha_{cr}}{\alpha_{cr}}+\dfrac{D_4}{D_3}k_{zp}\cos\alpha_{cr}\\ D_7=\dfrac{\sin\alpha_{cr}}{\alpha_{cr}D_6}+k_{zp}\dfrac{\cos\alpha_{cr}}{D_3D_6}\dfrac{\sin\alpha_{cr}-\alpha_{cr}\cos\alpha_{cr}}{\alpha_{cr}}\\ D_8=-\dfrac{k_{zp}}{D_3}[\dfrac{D_4}{D_6}\dfrac{\sin\alpha_{cr}}{\alpha_{cr}}-(1-\dfrac{D_4k_{zp}\cos\alpha_{cr}}{D_3D_6})\\ \qquad\dfrac{\sin\alpha_{cr}-\alpha_{cr}\cos\alpha_{cr}}{\alpha_{cr}}]\\ K=\dfrac{(\rho_{cr}-R_{con}D_1D_7)q}{(D_1+D_2)(D_1D_7-1)-D_1D_8}\end{cases}\tag{22}$$

Computing the compressive stress at the crown point of the arch with Eq. (17). According to Eq.(17), the hoop force N and the bending moment M at the crown point can be written as a function of the external pressure q. When the material at the crown point starts to be yielded, this external pressure q can be regarded as the buckling pressure P_{arch} of the arch. Therefore, when the compressive stress reaches a given value σ_{cr}

$$\sigma_{cr}=\sigma_y-\sigma_{max}\tag{23}$$

the buckling pressure P_{arch} of this arch is

$$\frac{N}{t_c}+\frac{6M}{t_c^2}=\sigma_{cr} \tag{24}$$

By substituting Eq. (17) into Eq. (24), the buckling pressure P_{arch} of this spring-supported arch can be obtained. Finally, the critical pressure of a flexible riser with a layer gap is obtained by

$$P_{cr}=P_{con}+P_{arch} \tag{25}$$

2.3 Contact position at collapse moment

If the position of the contact point (R_{con} and β_{cr}) at the collapse moment is determined, the geometry of the arch can be obtained by Eq. (10), followed by calculating the critical pressure using the above methods. However, this position is not easy to determine since it is decided by multiple factors, including the gap width and bending stiffness ratio between the outer and inner layers. In order to tackle this problem, a formula needs to be proposed to estimate the value of R_{con} at the collapse moment. This formula for R_{con} should meet the following rules:

1) R_{con} is approximate to the sum of carcass radius, gap width and initial deflection when the outer layer becomes infinitely rigid;

2) R_{con} is approximate to the sum of carcass radius, gap width and maximum horizontal displacement ω_{max} when the outer layer's stiffness approaches zero;

3) R_{con} is not affected by the stiffness of the outer layer when $g_w \geqslant \omega_{max}$.

Therefore, a formula is proposed as

$$R_{con}=R_c+g_w+\omega_0+(\omega_{max}-g_w)\left(\frac{g_w+\omega_0}{\omega_{max}+\omega_0}\right)^{\Phi_K},$$
$$0\leqslant g_w\leqslant\omega_{max} \tag{26}$$

where $\Phi_K=\frac{E_p}{E_c}\left(\frac{t_pR_c}{t_cR_p}\right)^3$, is the bending stiffness ratio[8].

The buckling pressure P_{arch} of the arch can be determined by continually decreasing the value of β_{cr} (from $\pi/2$ to 0) to make the bending moments of the attached and detached portions at the contact position equal to each other, as shown in Fig. 10. The bending moment for the detached portion can be calculated with Eq. (17). For the attached portion, the bending moment M_1 at the contact position is obtained by[12]

$$M_1=E_cI_c\left(\frac{1}{\rho_{cr}}-\frac{1}{R_{con}}\right) \tag{27}$$

Once M and M_1 are matched, the angle β_{cr} can be determined, as well as the buckling pressure P_{arch} of the arch.

A flowchart that shows the whole procedure is given in Fig. 11.

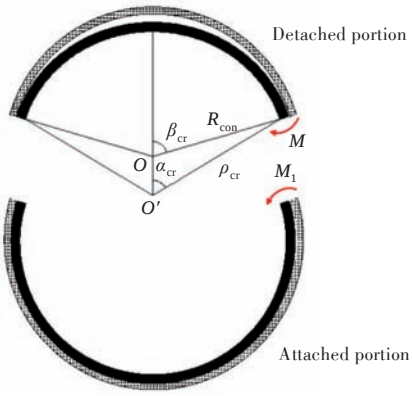

Fig.10 Bending moments at contact position

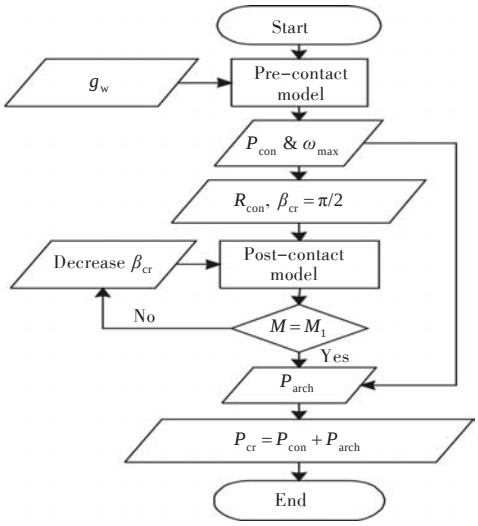

Fig.11 Flowchart of whole analysis procedure

The initial layer gap g_w is submitted to the pre-contact model to determine external pressure P_{con} for gap closure.

Once the carcass makes contact with the pressure armour, the spring-supported arch model (i.e. the post-contact model) is used. This arch model is initially assumed to have horizontal supports (i.e. β_{cr} = 90°), but its actual geometry at the collapse moment needs to be determined by decreasing arch angle β_{cr} to find bending moment equilibrium.

Once the geometry of this spring-supported arch is determined, its buckling pressure P_{arch} can be obtained. The collapse pressure for a flexible riser with a layer gap g_w is the sum of P_{con} and P_{arch}.

3 Verification

In order to verify the reliability of the proposed analytical model, finite element (FE) collapse models were built for comparison purposes. Since the carcass and pressure armour are layers with a laying angle close to 90°, they contribute little resistance to the tension or bending loads. Therefore, 2D FE models are mostly adopted to study the effects of geomet-

ric imperfection on the collapse of flexible pipes[8,16,22].

The 2D FE models were developed using Abaqus 6.13[22], the geometric and material data is listed in Table 1. Fig. 12 shows an overview of the mesh, applied load and boundary conditions of the FE model. More specifically, the pressure load and boundary conditions are as follows:

Table 1 Geometric and material properties of layers[22]

Parameter	Carcass	Pressure armor
Initial ovalization	0.2%	–
Gap width/mm	Var.	–
Internal diameter/mm	101.6	Var.
Layer equivalent thickness/mm	3.97	Var.
Young's modulus/GPa	192.5	207
Poisson ratio	0.3	0.3
Yield strength/MPa	600	600
Tangent modulus/MPa	2 000	10 483

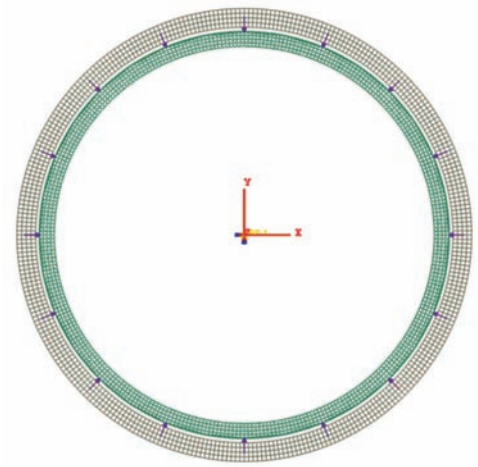

Fig.12 Loads and boundary conditions applied to finite element models

1) Pressure loads applied uniformly on the outer surface of the inner ring;

2) Symmetry conditions for the nodes on the x and y axes;

3) Ring centre fully fixed as a pilot node to restrain the free movement and rotation of the concentric ring model.

Three different wall thicknesses t_p of the outer layer (4, 5, 6 mm) were adopted in the case study. For each thickness, the gap width g_w between the inner and outer layers is 0.01, 0.05, 0.1, 0.2, 0.5 mm. Therefore, a total 15 cases were carried out for this paper. These cases were run by both the numerical and analytical models. Table 2 lists the numerical and analytical results of critical collapse pressure for all cases. Fig. 13 shows the typical collapse process of a flexible riser with an initial layer gap using the 2D FE models.

From the results listed in Table 2, it can be seen that the effect of gap width has significant influence on the anti-collapse strength of the carcass. The FE analysis shows that the reduction in the collapse pressure of the flexible riser caused by an initial layer gap is generally around 18% when it increases from 0 to 0.5 mm. For a carcass surrounded by a thicker pressure armour, the same level of layer gap causes a larger reduction in collapse pressure. This indicates that the layer gap reduces the collapse strength of the carcass by weakening the supporting effect of the surrounding pressure armour.

Additionally, the prediction of the analytical models agrees very well with that of the FE models when there is a small layer gap. For cases with a gap width

Table 2 Numerical and analytical results of critical pressure for each case

Wall thickness of pressure armour g_w /mm	Critical pressure at t_p=4 mm			Critical pressure at t_p=5 mm			Critical pressure at t_p=6 mm		
	Numerical /MPa	Analytical /MPa	Error /%	Numerical /MPa	Analytical /MPa	Error /%	Numerical /MPa	Analytical /MPa	Error /%
0.01	28.14	28.73	2.08	33.16	33.75	1.78	36.12	35.08	−2.9
0.05	27.47	28.01	1.95	32.34	32.19	−0.47	35.26	33.66	−4.53
0.1	26.74	27.25	1.91	31.42	30.64	−2.48	34.23	32.23	−5.84
0.2	25.82	25.99	0.67	29.83	28.26	−5.23	32.42	29.72	−8.34
0.5	23.07	22.81	−1.14	26.28	23.6	−10.19	28.54	24.22	−15.14

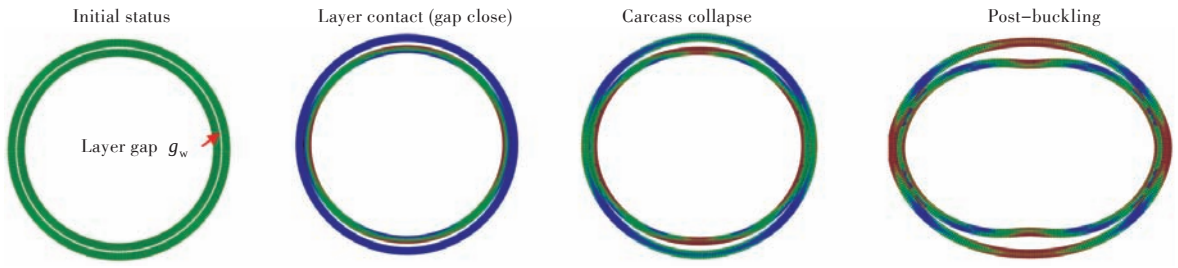

Fig.13 Collapse process of flexible riser simulated by 2D finite element model

close to zero, the errors are all smaller than 5%. However, the critical pressure predicted by the proposed models gradually deviates from the FE models results with the increase of gap width and outer layer thickness. For a concentric ring with a gap width of 0.5 mm and an outer layer thickness of 6 mm, the error can be higher than 15%.

The main cause of the above phenomenon is the assumption of thrust force adopted in the boundary conditions in Eq. (19). This assumption was proposed by Jacobson[21] for a pipe encased in a rigid circular cavity. However, the situation is different for a flexible riser as its pressure armour is not a rigid layer. In this situation, the thrust force at the contact position is governed by multiple factors, e.g. the ovality of the inner layer, gap width and stiffness ratio between layers. Therefore, this assumption gives a less accurate estimation of thrust force at the contact position for flexible risers with a larger gap width and thinner pressure armour. Finally, large deviations appeared for such cases.

4 Conclusions

A flexible riser is a key enabler of oil and gas production in ultra-deep water which transports production fluids between floaters and subsea wells, they are required to have sufficient collapse resistance for any abnormal condition of a flooded annulus, and the layer gap between the carcass and pressure amour has a significant reduction effect on the anti-collapse strength of flexible risers.To date, there few analytical models have been developed to address this issue. This paper proposes a spring-supported arch model that can predict the wet collapse pressure of a flexible riser with a layer gap. Numerical simulation was adopted to verify the reliability of the proposed model. The carcass and pressure armour were both considered as rings in these two kinds of models, with the assumption of an figure-eight-shaped collapse mode. The predictions of both models showed that collapse pressure is very sensitive to pressure amour stiffness and gap width. The anti-collapse strength of a tightly fitted carcass supported by stiffer pressure amour can be largely enhanced.

In addition, the proposed model gives a prediction in high agreement with the results of numerical simulation for a tightly fitted carcass. However, for a loosely fitted carcass, the accuracy of this model may decrease due to the assumption of thrust force used in the boundary conditions. The comparison results indicate that the proposed model can be a reliable tool for a flexible riser with stiffer pressure amour and a smaller layer gap.

References

[1] BAI Y, BAI Q. Subsea engineering handbook [M]. Houston, USA: Elsevier Inc., 2010.

[2] National Oilwell Varco. Floating production systems-dynamic flexible risers[R]. [S.l.]: NOV, 2014.

[3] DAG F, ARE L S. Handbook on design and operation of flexible pipes[R]. Trondheim: Norsk Marinteknisk Forskningsinstitutt AS, 2017.

[4] SAGLAR N, TOLEMAN B, THETHI R. Frontier deepwater developments-the impact on riser systems design in water depths greater than 3 000 m[C]//Proceedings of Offshore Technology Conference (OTC). Houston, Texas, USA: OTC, 2015.

[5] FERNANDO U S. Challenge and solutions in developing ultra-high-pressure flexibles for ultra-deep-water applications[R]. [S.l.]: GE Oil & Gas, 2015.

[6] NETO A G, MARTINS C A. Flexible pipes: influence of the pressure armor in the wet collapse resistance[J]. Journal of Offshore Mechanics and Arctic Engineering, 2014, 136(3): 031401.

[7] PAUMIER L, AVERBUCH D, FELIXHENRY A. Flexible pipe curved collapse resistance calculation [C]//Proceedings of the 28th ASME International Conference on Ocean, Offshore and Arctic Engineering. Honolulu, Hawaii, USA: ASME, 2009.

[8] BAI Y, YUAN S, CHENG P, et al. Confined collapse of unbonded multi-layer pipe subjected to external pressure[J]. Composite Structures, 2016, 158: 1-10.

[9] AXELSSON G, SKJERVE H. Flexible riser carcass collapse analyses: sensitivity on radial gaps and bending[C]//Proceedings of the 33rd ASME International Conference on Ocean, Offshore and Arctic Engineering. San Francisco, USA: ASME, 2014.

[10] DESOUSA J R M, PROTASIO M K, SAGRILO L V S. Equivalent layer approaches to predict the bisymmetric hydrostatic collapse strength of flexible pipes [C]//Proceedings of the 37th ASME International Conference on Ocean, Offshore and Arctic Engineering. Madrid, Spain: ASME, 2018.

[11] DAVIDSON M, FERNANDO U S, ODONNELL B, et al. Prediction of extruded profile shape of polymer barrier in flexible pipes[C]//Proceedings of the 26th International Ocean and Polar Engineering Conference. Rhodes, Greece: ISOPE, 2016.

[12] TIMOSHENKO S P T, GERE J M. Theory of elastic stability [M]. 2nd ed. New York, USA: McGraw-Hill Co., 1961.

[13] GLOCK D. Post-critical behavior of a rigidly encased circular pipe subject to external water pressure and thermal extension[J]. Der Stahlbau, 1977, 46(7): 212-217.

[14] BOOT J C. Elastic buckling of cylindrical pipe linings with small imperfections subject to external pressure

[J]. Tunnelling and Underground Space Technology, 1997, 12: 3–15.

[15] THÉPOT O. Structural design of oval–shaped sewer linings [J]. Thin–Walled Structures, 2001, 39: 499–518.

[16] CHEN Y G, LIU J, ZHU L F, et al. An analytical approach for assessing the collapse strength of an unbonded flexible pipe[J]. Journal of Marine Science and Application, 2015, 14(2): 196–201.

[17] LO K H, ZHANG J Q. Collapse resistance modeling of encased pipes[M]//ECKSTEIN D. Buried plastic pipe technology, Volume 2. West Conshohocken, PA: American Society for Testing and Materials, 1994.

[18] ELSAWY K M, SWEEDAN A M I. Elastic stability analysis of loosely fitted thin liners–a proposed simplified procedure and evaluation of existing solutions [J]. Tunnelling and Underground Space Technology, 2010, 25(6): 689–701.

[19] MARTINS C A, PESCE C P, ARANHA J A P. Structural behavior of flexible pipe carcass during launching[C]//Proceedings of the 22nd International Conference on Offshore Mechanics and Arctic Engineering. Cancun, Mexico: ASME, 2003.

[20] TONG G S. In plane stability of steel structures[M]. Beijing: China Architecture & Building Press, 2005 (in Chinese).

[21] JACOBSON S. Buckling of circular rings and cylindrical tubes under external pressure[J]. Water Power, 1974, 26: 400–407.

[22] MALTA E R, CLOVIS D A M, NETO A G, et al. An investigation about the shape of the collapse mode of flexible pipes[C]//Proceedings of the 22nd International Offshore and Polar Engineering Conference. Rhodes, Greece: ISOPE, 2012.

用于预测含层间间隙缺陷柔性立管的静水压溃强度的弹性支撑拱结构模型

李骁*, 江晓俐, Hopman Hans

代尔夫特理工大学 海事与运输技术系,荷兰 代尔夫特 2628 CN

摘　要:[**目的**]随着油气勘探涉入超深水领域,一旦柔性立管的外层结构发生破损,其内部的骨架层将承载巨大的外部水压。如果骨架层与铠甲层之间存在层间间隙,则将削弱骨架层的压溃强度,进而引发所谓的湿压溃。[**方法**]针对该问题,提出一种弹性支撑拱结构模型,并将骨架层的湿压溃过程分为接触前与接触后2个阶段。在接触之前,采用单环结构的稳定性理论分析内骨架层的失稳行为;当层间间隙闭合之后,骨架层开始受到铠甲层的支撑,该结构进入接触后阶段,此时外部铠甲层可以简化为径向支撑弹簧,用于支撑内部骨架层的分离拱状部分。基于此,建立有限元压溃模型,用以验证该解析模型的可靠性。[**结果**]2类模型的预测结果吻合良好,压溃压强对铠甲层刚度和间隙宽度均非常敏感;当初始层间间隙宽度由0增加至0.5 mm时,柔性立管的压溃压强将降低18%左右;如果紧密拟合的骨架由更硬的铠甲层支撑,则将大幅提高其抗压溃强度。[**结论**]对于具有较硬铠甲层和较小层间间隙的柔性立管而言,该解析模型可以有效预测其静水压溃强度。

关键词:柔性立管;临界压溃压强;层间间隙;湿压溃;超深水